

XAFS study of americium sorbed onto groundwater colloids

Claude Degueldre,^{a*} Donald Reed,^b A. Jeremy Kropf^b and Carol Mertz^b

^aNuclear Energy and Safety Division, Paul Scherrer Institute, 5232 Villigen, Switzerland, and ^bChemical Technology Division, Argonne National Laboratory, Argonne, IL, USA.
E-mail: claudedegueldre@psi.ch

The sorption of americium, as Am(III), onto groundwater colloids obtained from a marl aquifer was studied in $2 \times 10^{-2}M$ sodium bicarbonate groundwater and $2 \times 10^{-2}M$ sodium chloride bicarbonate-free solutions. At the *in situ* groundwater pH of 8.6, the americium was strongly sorbed onto the colloids. XAFS analyses were performed on these sorbed Am species to establish the oxidation state and its near-neighbour bonding. These XAFS data, obtained at 400 mg l^{-1} colloid concentrations and total Am concentration of $1.53 \times 10^{-5}M$ (dissolved and onto colloids), indicated that Am remains trivalent, and that surface complexes are formed with the colloids without surface precipitation. This conclusion is based on the absence of Am–Am interactions in the second or third shells. The surface complexes generated by the Am(III) sorbed onto active sites are described on the basis of the XAFS data. They include the presence of about seven water molecules around the ternary surface complexes of this trivalent actinide.

Keywords: XAFS; americium; sorption; colloids; marl; groundwater.

1. Introduction

The structure of Am(III) sorbed onto natural groundwater colloids from the Wellenberg aquifer has been studied in the presence and absence of carbonate. Americium, which is a several hundred-year half-life nuclide, is a transuranic contaminant present in radioactive waste. It is generally encountered in the trivalent form in groundwater under subsurface conditions. In this context, its subsurface chemistry, by analogy, has a broad implication for all safety-relevant trivalent radionuclides such as plutonium, curium and many lanthanides.

The key feature of this actinide study is the use of synchrotron-based methods, like those performed on actinide oxides, ions and oxy-ions by Conradson (1998), and on americium by Soderholm *et al.* (1997), Runde *et al.* (1997), Bonhoure (2000), Den Auwer *et al.* (2000) and Reed *et al.* (2003).

The sorption behaviour of actinides under quasi-neutral pH conditions is currently described using surface complexation models, which consider $>Al-OH$, $>Si-OH$ and $>Fe-OH$ as active sites at the surface of the natural aquifer particles. This work complements and expands the sorption study performed by radiochemical tests and published recently (Degueldre *et al.*, 2001) based on the characterization of these groundwater colloids reported earlier (Degueldre *et al.*, 1999).

Groundwater colloids can play a key role in the subsurface migration of actinides. Penrose *et al.* (1990) observed that Pu and Am were transported in groundwater for at least 3.4 km down-gradient from a discharge at the Los Alamos site in New Mexico. Degueldre *et al.* (1996) also demonstrated that rare-earth elements, which are analogous to americium and uranium, were transported over distances of several km in granitic fissures at the Menschenschwand uranium mine, Germany. Litaor *et al.* (1998) demonstrated that americium- and plutonium-contaminated suspended particles migrated in the subsurface over distances of the order of 100 m in 30 years at Rocky Flats, Colorado. Kersting *et al.* (1999) found that groundwater colloids transported plutonium over a distance of 1.4 km in about 30 years at the Nevada Test Site.

The overall importance of subsurface colloidal transport, however, is not resolved since there are studies that show that colloids do not migrate. A good example of this is the Morro do Ferro study (Miekeley *et al.*, 1992), where rare-earth-associated colloids did not migrate in the Brazilian system. This unresolved question and the relevance of potential contaminant transport by a colloid-facilitated mechanism make it important to obtain data on groundwater colloid properties to properly assess and predict contaminant migration.

The overall importance of subsurface colloidal transport, however, is not resolved since there are studies that show that colloids do not migrate. A good example of this is the Morro do Ferro study (Miekeley *et al.*, 1992), where rare-earth-associated colloids did not migrate in the Brazilian system. This unresolved question and the relevance of potential contaminant transport by a colloid-facilitated mechanism make it important to obtain data on groundwater colloid properties to properly assess and predict contaminant migration.

2. Experimental

2.1. Wellenberg groundwater and colloids

The groundwater and colloids were extracted from the Wellenberg site in central Switzerland (Degueldre *et al.*, 1999). The groundwater was sampled through an artesian borehole equipped with a double packer and a PVC line. The water is a $2 \times 10^{-2}M$ sodium bicarbonate fluid with an *in situ* pH of 8.6 and with a low calcium concentration ($4 \times 10^{-5}M$). The rock is composed of 45% calcite, 8% dolomite/ankerite, 14% quartz, 10% smectite, 10% illite and 8% chlorite. The colloid composition is 35% smectite, 35% illite and 30% chlorite (Degueldre *et al.*, 1999).

Prior to their use, the groundwater colloids were concentrated from the original groundwater (colloid concentration about 0.1 mg l^{-1}) by tangential filtration utilizing a low cut-off (5 nm) membrane. 1 l of concentrate was obtained from 20 l after an enrichment factor of 20. It was diluted in 1 l ultra-pure water to avoid significant aggregation. The 2 l of concentrate (about 1 mg l^{-1}) was further processed by centrifugation 25 ml at a time for 20 min at $\sim 4000 \text{ g}$. For each concentration step, only 20 ml of the supernatant were discarded leaving 5 ml of the groundwater with the colloids. These 5 ml were re-suspended in 20 ml of colloid-free water using vortex and ultrasonic treatments. Two 25 ml samples were obtained, with colloid concentrations of the order of 400 mg l^{-1} . The first one was used as produced after re-suspending in colloid-free water. The second one was centrifuged for 15 min at $\sim 4000 \text{ g}$; 20 ml were discarded and the 5 ml colloid concentrate was re-suspended in 20 ml of $2 \times 10^{-2}M$ NaCl solution. This procedure was repeated a second time. The final colloid solution was also $\sim 400 \text{ mg l}^{-1}$ and its bicarbonate concentration was about $10^{-5}M$; the pH was re-adjusted to 8.6 using either hydrochloric acid or sodium hydroxide.

The dynamic light scattering (DLS) apparatus used in this study consisted of a Malvern 4700c Photon Correlation Spectrometer fitted with a Uniphase argon ion laser (514.5 nm, 3–75 mW). Performance of the instrument was checked with a series of polystyrene size standards (nominal sizes of 100 and 300 nm) from the National Institute of Standards and Technology (Gaithersburg, MD, USA). The size standards were prepared in filtered deionized water according to certification instructions. Unfiltered sample aliquots were taken for DLS measurements and placed in a temperature-controlled water bath (298 K). Data were collected at 3 mW and a scattering angle of 90° . Data analysis was performed using the commercial software routine *Contin* (e.g. Stock & Ray, 1985), which involves LaPlace inversion of the correlation function. The single-

Table 1
Sorption conditions for both bicarbonate and bicarbonate-free batches.

Conditions	Bicarbonate	Sodium chlorite
Water type	Wellenberg water	Salt water
Solution	$2 \times 10^{-2} M$ NaHCO ₃	$2 \times 10^{-2} M$ NaCl, $\sim 10^{-5} M$ HCO ₃
pH	8.6 ± 0.2	8.6 ± 0.4
Eh	Oxidizing	Oxidizing
Colloid concentration	~10 mg in 25 ml	~10 mg in 25 ml
Am amount added	100 µg in 2 h	100 µg in 2 h
pH check after addition	Correction with HCl/NaOH	Correction with HCl/NaOH
Contact time	2 h after pH correction	2 h after pH correction

particle counting (SPC) data obtained for the original groundwater colloids were obtained using a PMS unit as reported earlier (e.g. Degueldre *et al.*, 1996).

2.2. Americium sorption experiments

A summary of our experimental conditions for sorption experiments is given in Table 1 for both the bicarbonate and bicarbonate-free solutions. The americium-241 starting solution was $1.68 \times 10^{-4} M$ Am(III) perchlorate (17 ml, pH 3). The initial absorption spectrum was obtained on a Varian CARY-5 spectrometer to verify its solution speciation.

The Am(III) stock solution was added to the Wellenberg colloids in groundwater and sodium chloride solutions in a stepwise fashion, very slowly and under extensive stirring to minimize the potential precipitation of Am phases. The sorption was carried out in a 25 ml batch with the addition (every 10 min) of ten successive spikes of 250 µl of Am(III) stock solution. The final americium concentration, sorbed and dissolved, was $1.53 \times 10^{-5} M$, with at least 70% of the americium present as sorbed species. The concentration of dissolved Am was much smaller ($\sim 5 \times 10^{-7} M$) (see Degueldre *et al.*, 2001). The pH of each solution was re-checked after the addition of the americium to verify that no change had occurred.

Separation was performed by filtration in an Amicon minicell with 100 nm pore Nuclepore membranes under a 2×10^5 Pa N₂ atmosphere. Three filtrations were carried out with the fluid of the 25 ml colloid batch, and the three membranes, loaded with colloid cake, were mounted in sandwiches for XAFS investigations.

Liquid scintillation counting was used to determine the specific activity of the solution using a 10 µl sample and 15 ml scintillation cocktail. The liquid scintillation unit was a Packard model 2500 TR liquid scintillation analyser.

2.3. XAFS analysis of sorbed Am colloids

The colloid-loaded membranes were stacked in the sample carrier and mounted in a triply encapsulated configuration, which is a standard approach (Richmann *et al.*, 2002) for radioactive samples. The XAFS measurements were performed on the Materials Research Collaborative Access Team line (MR-CAT) at the Advanced Photon Source (APS), Argonne National Laboratory. The energy was calibrated using a Zr foil (first inflection, 17998.4 eV), as well as by assigning the white-line maximum of a uranyl nitrate hexahydrate sample to 17178 eV. Owing to the indirect nature of the calibration and the energy separation of the Am L_{III} edge from these two references, the energy scale is only accurate to ±2 eV.

The MR-CAT uses a cryogenically cooled, double-crystal Si(111) monochromator in conjunction with a Pt-coated mirror to minimize the presence of harmonics. The incident-intensity ionization chamber was filled with nitrogen gas, while the transmission ionization chamber was filled with a mixture of gases, nitrogen with 30% Ar.

The fluorescence ionization chamber had a path length of 3 cm and was filled with Xe gas. The sample was mounted at 45° relative to the incident beam and the detector. The data for each sample are the sum of eleven 4 min scans. The data were processed using the *UW* analysis package for background removal and normalization (Ravel, 2001), *FEFFIT* for multiple-shell fitting (Stern *et al.*, 1995) and *FEFF* (version 8.0) for calculating the scattering paths for various models (Ankudinov *et al.*, 1998).

3. Results and discussion

3.1. Colloid characterization and effective sorption coefficient

The groundwater colloids from the 400 mg l⁻¹ concentrate used in the sorption study were examined using DLS. This colloid suspension, which was too concentrated for DLS measurements, was diluted to obtain a 16 mg l⁻¹ colloidal solution. This colloid sample was measured with DLS and a mean diameter of 220 nm (mode of 160 nm) was measured with a distribution width of 340 nm (Fig. 1a). In contrast, the colloid size distribution of the original Wellenberg groundwater indicated a mean diameter of about 70 nm (Fig. 1b). The distribution of the concentrate was widely dispersed but the maximum in the relative distribution was biased towards larger sizes owing to local aggregation. This bias effectively decreases the specific sorption activity of the colloids utilized in the Am study, possibly leading to reduced sorption coefficient (*K_d*) measurements.

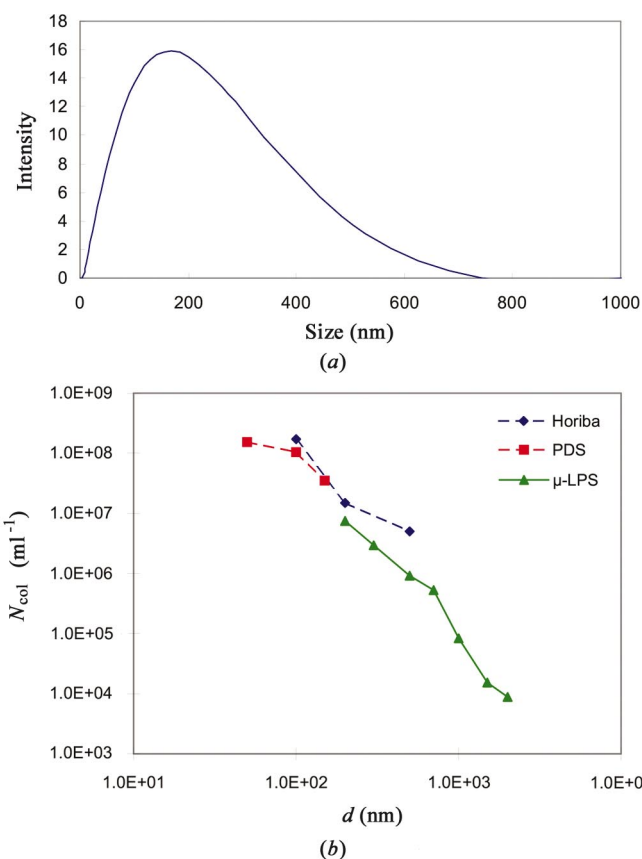


Figure 1
Wellenberg colloid size distributions for (a) 4% concentrate obtained using DLS, and (b) in groundwater using SPC (Degueldre, 1997; Degueldre *et al.*, 1999), ■, ▲ and ◆ for the three units utilized on line.

Table 2

Americium sorption yield on the studied colloids and corresponding Kd values.

Fluid conditions	Wellenberg groundwater	Sodium chloride solution
Solution, pH = 8.6	$2 \times 10^{-2} M$ NaHCO ₃	$2 \times 10^{-2} M$ NaCl, $\sim 10^{-5} M$ HCO ₃
Sorption yield (%)	72.0	99.4
Kd^\dagger values (ml g ⁻¹)	6.4×10^4	4.2×10^6

[†] Assuming equilibrium as discussed in Degueldre *et al.* (2001).

For a mean diameter of 200 nm the volume of one colloid is 8×10^{-15} cm³, or a mass of 1.6×10^{-14} g, which corresponds to about 10^{12} particles for a 10 mg batch. The surface of one spherical colloid is around 2.5×10^{-9} cm² and the total surface of the 10 mg colloid is 2.5×10^3 cm². Assuming a site density of 3 sites nm⁻², the number of sites on the 10 mg of colloid is 7.5×10^{17} , corresponding to 10^{-6} moles of sites. This corresponds to a maximum of 240 µg of Am which is well above the amount utilized, *i.e.* 100 µg Am. These sites are either strong or weak surface complexation sites and, for this pH, sorption may be performed by both processes according to the concentration of the actinide. The americium sorption data are reported in Table 2. During sorption the concentrations are always below the solubility limits of americium hydroxide or carbonate under the investigated conditions (Degueldre *et al.*, 2001).

3.2. XAFS analysis of sorbed Am

The XANES spectra of Am sorbed on Wellenberg colloids are shown in Fig. 2 for the groundwater and sodium chloride solutions. The Am edge position is the same for the two colloid samples and is 18503 ± 2 eV based on the half-height analysis. The XANES obtained are most consistent with an Am(III) oxidation state. The edge position measure agrees with that reported elsewhere (Williams *et al.*, 2000), although given the difference in calibration schemes this is not viewed as a conclusive indication of the oxidation state. It also matches the Am(III) XANES shape when compared with the published spectra for [AmP₅W₃₀O₁₁₀]¹²⁻ and AmF₃ reported by Williams *et al.* (2000). The white line in our data is slightly sharper, most likely due to the improved monochromator resolution of an insertion-device beamline.

Some theoretical arguments suggest that Am(IV) is not formed by coupled sorption and redox amphotization by surface complexation. On the basis of the pH-Eh diagram for Am reported by Brookins (1990), which presents a stability domain for Am(IV) under neutral and oxidizing conditions, it was originally hypothesized that Am(III) may be oxidized in water to Am(IV) during sorption under neutral conditions. This behaviour, with regards to sorption, was revisited on the basis of the work performed earlier, coupling surface complexation and hydrolysis (Degueldre *et al.*, 1994) and combining redox (Degueldre, 1995), using the best thermodynamic data available for Am. It was calculated that Am(III) should not undergo redox changes during sorption by surface complexation under our experimental conditions. The XANES data and the modelling results support the conclusion that Am(III), not Am(IV), is sorbed on the Wellenberg colloids.

A second key result is that the XAFS of the sorbed Am was nearly identical in both samples (Fig. 2a) although the aqueous speciation of Am(III) was very different (*i.e.* carbonate *versus* hydrolysis). This is demonstrated by the EXAFS data shown in Fig. 2(b). The k^3 -weighted data were fit between $k = 2.5$ and 10.0 \AA^{-1} . A modified Hanning window function, rolled off over 1.0 \AA^{-1} , was used to reduce

Fourier-transform-induced artefacts. Three scattering paths were used to model the data between 1.2 and 3.5 Å: the first path was an Am–O path, the second an Am–X path with X either Fe or Si/Al, and the third a long Am–O path. The scattering paths were generated by FEFF using self-consistent potentials, which resulted in more accurate Fermi energies. The coordination numbers and radial distances were allowed to vary for all paths, while the EXAFS Debye–Waller factor (σ^2) was only allowed to vary for the first Am–O path, owing to instability in σ^2 for the second- and third-neighbour paths caused by interference of the two paths as well as the nearest-neighbour path. The amplitude reduction factor, S_0^2 , was fixed at 0.9 in the absence of any known Am standards to use as a calibration. One ΔE_0 value was used globally for all of the paths. This resulted in a maximum of eight variables. Based on the data ranges used (Δk and ΔR), up to 13 variables would be allowed.

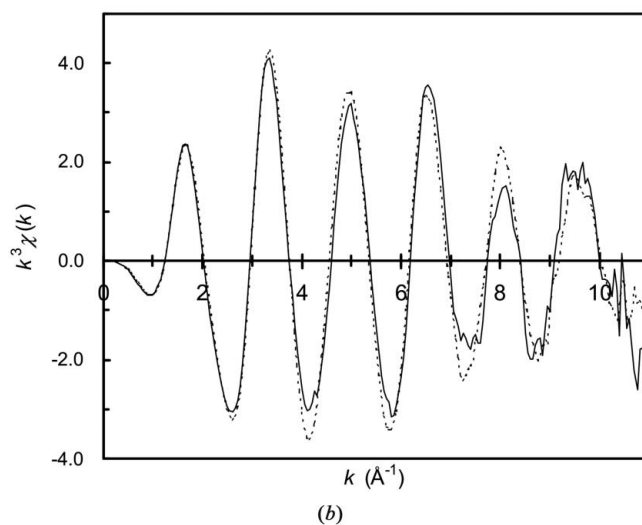
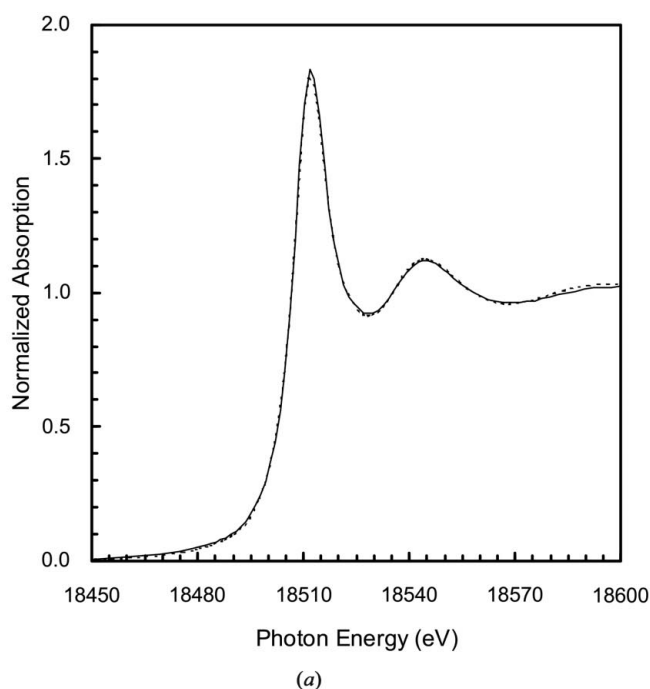


Figure 2
(a) XANES of Am sorbed onto Wellenberg colloids in $2 \times 10^{-2} M$ sodium bicarbonate (dashed line) and bicarbonate-free $2 \times 10^{-2} M$ sodium chloride (solid line) solution. (b) The isolated k^3 -weighted EXAFS data are shown.

Table 3

Stereochemical data.

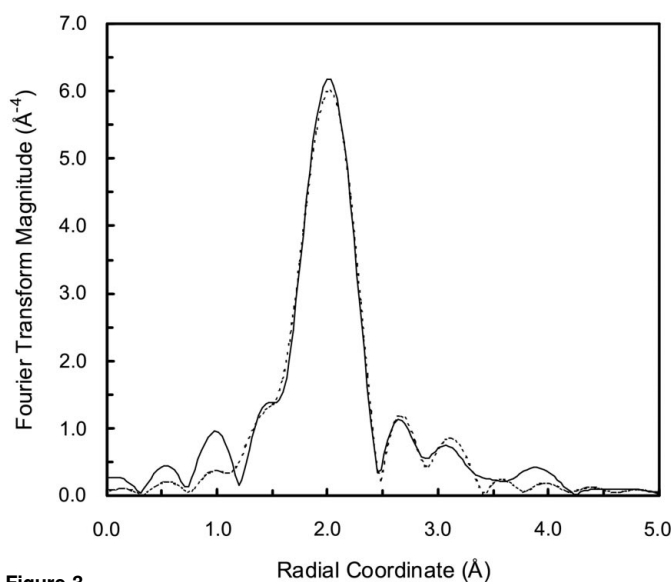
 N : coordination number; R : distance; σ^2 : Debye–Waller factor; ΔE_0 : relative energy threshold.(a) For Am (Am^{3+} ionic radius of 1.07 Å) and La (La^{3+} ionic radius of 1.02 Å) in selected compounds

Compound	Path	N	R (Å)	Reference
AmOCl	≡Am–O–	4	2.34	ICSD (1999)
AmOBr	≡Am–O–	4	2.42	ICSD (1999)
AmOI	≡Am–O–	4	2.76	ICSD (1999)
Am ₂ O ₃	≡Am–O–	6–6	2.37–4.43	ICSD (1999)
AmO ₂	≡Am–O–	8	2.33	ICSD (1999)
La ₂ (CO ₃) ₃ · 8 H ₂ O	≡La–O–	2–2–2–2	2.54–2.63–2.66–2.73	ICSD (1999)
La ₂ (CO ₃) ₃ · 8 H ₂ O	≡La–C≡	1–4–2	2.94–3.05–3.63	ICSD (1999)
LaOHCO ₃	≡La–O–	1–1–2–2–2	2.47–2.49–2.58–2.59–2.65	ICSD (1999)
LaAlO ₃	≡La–Al≡	2–6	3.27–3.28	ICSD (1999)
LaFeO ₃	≡La–Fe≡	2–2–2–2	3.27–3.38–3.43–3.54	ICSD (1999)
La ₂ Si ₂ O ₇	≡La–Si≡	1–1–2–1–1	3.27–3.44–3.49–3.54–3.75	ICSD (1999)

(b) Am experimental data

Sample	Path	N	R (Å)	σ^2 ($\times 10^{-3}$ Å ²)	ΔE_0 (eV)
Bicarbonate	≡Am–O	11.0 ± 0.9	2.50 ± 0.02	10.3 ± 1.0	2.1 ± 0.6
	≡Am–Si/Al≡	1.1 ± 0.5	3.11 ± 0.03	8.0	
	≡Am–O	3.3 ± 1.3	3.51 ± 0.04	10.0	
Bicarbonate-free	Am–O	10.3 ± 1.3	2.50 ± 0.02	10.9 ± 1.9	2.1 ± 0.8
	≡Am–Si/Al≡	1.5 ± 0.6	3.12 ± 0.03	8.0	
	≡Am–O≡	4.3 ± 2.0	3.54 ± 0.04	10.0	

The magnitude of the Fourier transform along with the fit for the bicarbonate-free sample are shown in Fig. 3. These data resemble the data published earlier by Runde *et al.* (1997) for $\text{Am}^{3+}(\text{aq})$ in 1M HClO₄. The fit parameters derived from this analysis are given in Table 3. The interatomic distances in selected Am and La compounds are given for comparison. The nearest neighbour (nn) corresponds to an Am–O distance of 2.50 ± 0.02 Å with a coordination of 11. This bond distance is consistent with trivalent Am compounds (*e.g.* Soderholm *et al.*, 1996). The high coordination suggests also the presence of water molecules as part of a solvation shell, hydroxyl group(s) and/or carbonyl O atoms complexed to the Am.

**Figure 3**

Radial distribution function obtained for the L_3 edge of Am observed after sorption on Wellenberg groundwater colloids for the 2×10^{-2} M bicarbonate solution (solid line) and a fit (using FEFFIT) to the data (dashed line). No Am–Am signal was observed from these EXAFS data corresponding to single-adsorbed species rather than precipitates.

The second-neighbour atom was Al or Si with a bond distance of 3.11 ± 0.03 Å and a coordination of approximately 1. This bond correlates reasonably with the range La–Al or La–Si. Iron was eliminated as a possible site atom because of the lower fraction of iron in the colloidal phase and because the second shell can only fit well with an Am–Fe scattering path of 2.86 Å, which is too short. There are two important observations about the second-shell data. First, there is little possibility of determining whether a carbon atom is present in the ternary surface complex, as expected if a carbonate is present as ligand. This is because the Am–C path is hidden in the data owing to the difference of one oxygen ligand between the two samples, and this contribution is so small (as calculated by simulation for the two types of surface complex) that it does not result in a significant difference in the spectra. Second, the second-shell fit also shows that the presence of Am atoms owing to the precipitation at the surface is unrealistic, since there is no Am–Am scattering path. This confirms that an insignificant amount of precipitation occurred during the preparation of the samples and that Am is truly sorbed to the surface of the Wellenberg colloids.

The third shell was fit with an Am–O path giving a distance of 3.52 ± 0.04 Å and a coordination of 3 or 4. These may be the Si/Al oxygen moieties on the colloid. These data are somewhat speculative since the presence of hydration water molecules and light elements in the second shell make the signal too weak to support detailed conclusions about the third-shell structure.

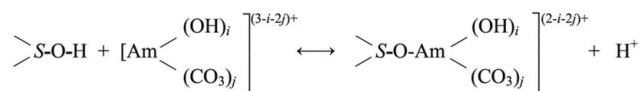
3.3. Discussion of the sorption data

The XAFS data obtained in this study provide some important insights about the nature of the sorbed species. First, the sorption of the Am(III) species on Wellenberg colloids does not result in the oxidation of americium to an Am(IV) species. As discussed earlier, the Am edge does not shift towards an Am(IV) position and the XANES spectra resemble those published for Am(III) compounds. Second, the presence of Am(IV) surface complexes would lead to shorter Am–O bonds, as suggested in Table 3 with Am–O bonds of 2.33 Å.

The sorption of the Am(III) species onto model colloids was recently revisited by Alonso & Degueldre (2003) using thermodynamic models. The authors showed that for the studied pH conditions the surface complexes of americium do not oxidize even under oxidizing conditions.

The second-shell analysis eliminates the iron site as the predominant sorption site; however, it is impossible to distinguish between Al and Si, and both sites remain potential sorption sites. Third, it is difficult to determine if carbon atoms are present in the second shell. If carbonates are absent from the surface complexes, that would reflect local pH changes. Lastly, there are no Am–Am peaks in the XAFS spectra suggesting the absence of Am surface precipitation on the colloids.

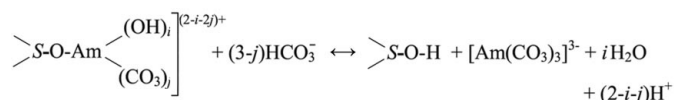
The modelling of the sorption of americium on these clay colloids can be schematized by surface complexation reactions such as:



where i or $j = 0, 1$ or 2 , and S represents either Al or Si, and where O–Am may be a strong or weak bond according to the nature of >S–O–H. It is currently observed that strong sites are first occupied at low-sorbing-species concentrations followed by the occupation of weak sites at higher concentrations.

The reactions imply that there is enough sorption capacity provided by the edge sites of the clay colloids. Presently, only the micromole per gram colloid is expected for the edge (strong site) sorption capacity while the weak site capacity implies that the basal sites may reach millimole values per gram colloid. In fact, for the clay colloid, both sites are active and both sorption mechanisms are possible. In addition to the inorganic ligands in these complexes, several water molecules participate in the coordination chemistry of the Am^{3+} ion.

Correspondingly, a desorption reaction may be written as follows:



which reduces the sorbing fraction of americium in bicarbonate solution as reported in Table 2. The fraction of Am sorbed is reduced, consequently decreasing the K_d value.

With a surface complex on a strong site, the Am–O bond should be expected to be shorter (*e.g.* 2.34–2.37 Å, see Table 3) than that observed (2.50 Å). The hypothesis implying a surface complex with a weak site is realistic. In this type of surface complex, >Al–O–Am(OH)₂·7H₂O or >Al–O–Am(CO₃)₂·7H₂O, all distances Am–O are apparently the same (from both the bicarbonate and bicarbonate-free precursor solutions). The data fitting from Fig. 3 resembles that published earlier by Runde *et al.* (1997) for Am^{3+} (aq) in 1M HClO₄. A similar result is observed by time-resolved laser fluorescence spectroscopy for Cm(III) sorption on alumina (Stumpf, Rabung *et al.*, 2001), kaolinite or smectite (Stumpf, Bauer *et al.*, 2001). In all these cases the sorbed Cm is only hydrated by four to five water molecules. In these studies the sorption is carried out at 3×10^{-7} M Cm, which induces the formation of strong surface complexes and the association of four to five water molecules around Cm. In this XAFS study the Am concentration is two orders of magnitude larger, inducing the formation of weak surface complexes with a larger number of hydration water molecules. This idea is supported by the recent results of the XAFS study reported by Dähn *et al.* (2002) for the sorption of Th(IV) on silica. This study demonstrated that waters

of hydration change from 5.8 to 8.6 when the Th concentration increases from the $\mu\text{mol g}^{-1}$ level to the $100 \mu\text{mol g}^{-1}$ level. This suggests a change from strong to weak sites when the actinide concentration increases. Consequently, the number of hydration water molecules in the surface complexes increases. The coordination-chemistry results derived from this study are illustrated in Fig. 4 with a structural molecular drawing obtained by using the distances and coordination numbers, and by using CHEMDRAW7.0 (ChemOffice 2002). This figure depicts a hydrated americium dihydroxo surface complex and shows that, thanks to its large size, Am(III) can be surrounded by seven water molecules. A similar figure could be drawn with the americium carbonate surface complex where the carbonate bidentate ion would replace the two-hydroxo ligands.

4. Conclusions

The sorption of Am(III) on groundwater colloids from a marl aquifer was studied in 2×10^{-2} M sodium bicarbonate (groundwater) or sodium chloride (bicarbonate-free) solutions. In these solutions the Am is strongly sorbed to the colloids at the *in situ* pH of 8.6. The XAFS analyses of the sorbed Am show that americium remains trivalent, that surface complexes (nearest neighbour at 2.50 Å, number of nearest neighbours = 10) form on the colloids without surface precipitation. This conclusion is based on the absence of Am–Am interaction in our XAFS spectra. The surface complexes generated by the Am(III) sorption on active sites, on the basis of the XAFS data recorded and the coordination chemistry of this trivalent actinide, involved a surface complex on sil–aluminol groups of Am hydroxocarbonato complexes. These surface complexes involve a rather high number of hydration water molecules. The site may consequently be a weak site from which decomplexation is possible

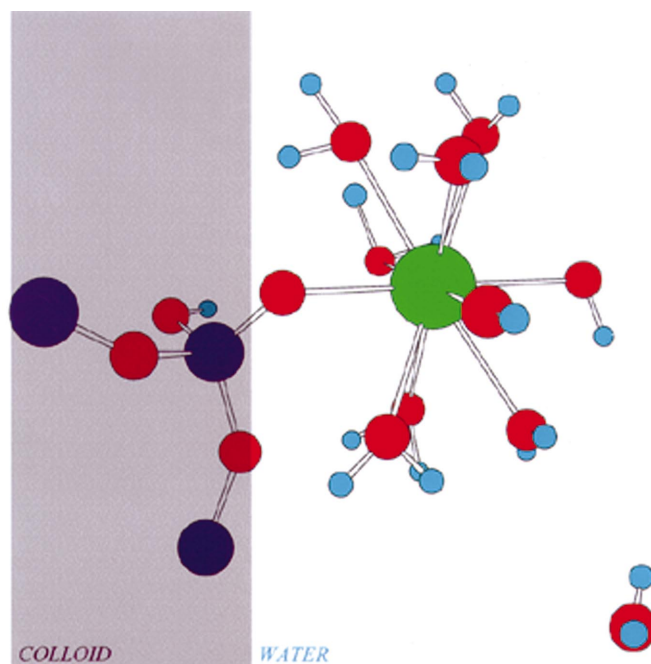


Figure 4 Am sorption schematic obtained by using the experimental data (distances and coordination numbers from Table 3) and applying the code CHEMDRAW for the hydrated Am(III) dihydroxo-complex sorbed on a Al/Si–O site on a colloid. Key to atoms: green, Am(III); light blue, H; dark blue, Al/Si; red, O.

by addition of bicarbonate and formation of soluble carbonate complexes.

The authors wish to acknowledge Scott Aase (CMT) for help in the preparation of the Am samples. Use of the Advanced Photon Source was supported by the US Department of Energy, Basic Energy Sciences, Office of Science, under Contract No. W-31-109-Eng-38. Work performed at MR-CAT is supported, in part, by funding from the Department of Energy under grant No. DEFG0200ER45811. At PSI, Enzo Curti is acknowledged for data research in ICSD. The colloid project for the program Nuclear Waste Management at PSI is partially funded by the National Cooperative of the Disposal of Radioactive Waste.

References

- Alonso, U. & Degueldre, C. (2003). *Collect. Surf. A*, **217**, 49–54.
- Ankudinov, A. L., Ravel, B., Rehr, J. J. & Conradson, S. D. (1998). *Phys. Rev. B*, **58**, 7565–7576.
- Bonhoure, I. (2000). Thesis, University of Paris XI, Orsay, Paris, France.
- Brookins, D. (1990). *Eh-pH Diagrams for Geochemistry*. New York: Springer-Verlag.
- Conradson, S. (1998). *Appl. Spectrosc.* **52**, 252A–279A.
- Dähn, R., Scheidegger, A., Manceau, A., Curti, E., Baeyens, B., Bradbury, M. & Chateigner, D. (2002). *J. Colloid Interface Sci.* **249**, 8–21.
- Degueldre, C. (1995). *J. Environ. Radioact.* **29**, 75–87.
- Degueldre, C. (1997). *Mater. Res. Soc. Symp. Proc.* **465**, 835–845.
- Degueldre, C., Bilewicz, A., Hummel, W. & Loizeau, J. L. (2001). *J. Environ. Radioact.* **55**, 241–253.
- Degueldre, C., Pfeiffer, H. R., Alexander, W., Wernli, W. & Brüttsch, R. (1996). *Appl. Geochem.* **11**, 677–695.
- Degueldre, C., Scholtis, A., Pearson, F., Laube, A. & Gomez, P. (1999). *Eclogae Geol. Helv.* **92**, 105–114.
- Degueldre, C., Ulrich, H. J. & Silbi, H. (1994). *Radiochim. Acta*, **65**, 173–179.
- Den Auwer, C., Charbonnel, M., Drew, M., Grigoriev, M., Hudson, M., Iveson, P., Madic, C., Nierlich, M., Presson, M., Revel, R., Russel, M. & Thuéry, P. (2000). *Inorg. Chem.* **39**, 1487–1495.
- ICSD (1999). *Inorganic Crystal Structure Database*. Fachinformationszentrum Karlsruhe, D-76344 Eggenstein-Leopoldshafen, Germany.
- Kersting, A., Efur, D., Finnegan, D., Rokop, D., Smith, D. & Thompson, J. (1999). *Nature (London)*, **397**, 56–59.
- Litaor, M., Barth, G., Ziba, E., Litus, G., Moffitt, J. & Daniels, H. (1998). *J. Environ. Radioact.* **38**, 17–46.
- Miekeley, N., Coutinho de Jesus, H., Porto da Silveira, C. & Degueldre, C. (1992). *J. Geochem. Explor.* **45**, 409–437.
- Penrose, W., Polzer, W., Essington, E., Nelson, D. & Orlandini, K. (1990). *Environ. Sci. Technol.* **24**, 228–234.
- Ravel, B. (2001). *J. Synchrotron Rad.* **8**, 314–316.
- Reed, D. T., Kropf, A. J., Aase, S. B., Degueldre, C., Curtiss, L. A., Zygmunt, S. A., Songkasiri, W. & Rittmann, B. E. (2003). *J. Nucl. Mater.* Submitted.
- Richmann, M. R., Reed, D. T., Kropf, A. J., Aase, S. B. & Lewis, M. A. (2002). *J. Nucl. Mater.* **297**, 303–312.
- Runde, W., Neu, M., Conradson, S., Clark, D., Palmer, P., Reilly, S., Scott, B. & Tait, C. (1997). *Mater. Res. Soc. Symp. Proc.* **465**, 693–703.
- Soderholm, L., Skanthakumar, S., Staub, U., Antonio, M. & Williams, C. (1997). *J. Alloys Compds*, **250**, 623–626.
- Soderholm, L., Williams, C., Skanthakumar, S., Antonio, M. R. & Conradson, S. (1996). *Z. Phys. B*, **101**, 539.
- Stern, E. A., Newville, M., Ravel, B., Yacoby, Y. & Haskel, D. (1995). *Physica B*, **208/209**, 117–120.
- Stock, R. S. & Ray, W. H. (1985). *J. Polym. Sci.* **23**, 1393–1447.
- Stumpf, Th., Bauer, A., Coppin, F. & Kim, J. I. (2001). *Environ. Sci. Technol.* **35**, 3691–3694.
- Stumpf, Th., Rabung, Th., Klenze, R., Geckeis, H. & Kim, J. I. (2001). *J. Colloid Interface Sci.* **238**, 219–224.
- Williams, C. W., Antonio, M. R. & Soderholm, L. (2000). *J. Alloys Compds*, **303/304**, 509–513.